J. Phys. UTM. Vol. 3. (2008) 109-118

A LASER PHOTOACOUSTIC IMAGING TECHNIQUE FOR THE DETECTION OF SMALL OBJECTS EMBEDDED IN TISSUE

[1]Jasman Zainal and [2]R J Dewhurst

[1]Physics Department, Faculty of Science
University Teknologi Malaysia, 81310 UTM Skudai, Johor, Malaysia
[2]School of Chemical Engineering and Analytical Science
The University of Manchester, Sackville Street, P.O.Box 88
Manchester M60 1QD
Email: jbz@dfiz2.fs.utm.my

ABSTRACT

We have applied a non-invasive photoacoustic technique to produce two-dimensional images of objects visually hidden within biological tissue. The technique has a foreseeable application for diagnosis of skin and subcutaneous diseases. We used a forward looking photoacoustic probe that integrated an optical-fibre laser pulse delivery system with a polymer transducer (PVDF) as a sensing element. The system's frequency response was in the few MHz regions. The probe was designed to transmit laser pulses and detect returning ultrasonic waves from features within tissue. Tissue sample were prepared using fresh chicken breast. They contained a strand of human hair or hairs threaded into the chicken breast near the surface, serving as a foreign body. B-scan studies under normal saline solution were performed by scanning the PVDF probe across the chicken breast. Results revealed an image of the hair or hairs with a lateral resolution down to ~ 500μm and depth resolution of about ~80μm. Some images not only showed the presence of a foreign body within the tissue, but they also contained photoacoustic features that may indicate the cross-sectional dimension of a human hair.

Keywords: Photoacoustics, PVDF, laser-ultrasound, B-scan imaging

INTRODUCTION

In recent years, advances in technology for clinical applications have improved the capability of detection and staging of cancerous tumours. Most of the efforts have been directed towards establishing diagnoses of clinically evident cancers. Several imaging modalities are sometimes limited by their inability to detect a small anomaly in tissue. Imaging techniques, such as magnetic resonance imaging, x-ray computerized tomography and ultrasound are in most cases only able to detect lesions with a size in excess of 0.5 cm diameter [1]. On some situations, non-invasive technique for early detection of cancer development is very desirable.

Photoacoustic theory has been discussed in several literature reviews eg. [2-5]. A photoacoustic (PA) technique offers an excellent alternative from a diagnostic perspective as it visualises semi-transparent biological tissue, exploiting optical contrast with ultrasonic resolution. Due to any differences in optical absorption within tissue [6], differences in the structure of tissue may be studied. The generation and detection of broadband photoacoustic transients may be used for on-axis monitoring of optically different structures in the interior of diffuse bodies such as biological tissue [7]. This has the potential to make photoacoustic techniques a new modality for clinical diagnosis. For example, at a specified wavelength of light, the absorption coefficient of blood can be 10 times higher than that of its surrounding tissues [8]. Because fast developing tumors consume more blood, most malignant tumors have higher optical absorption. Absorption contrast between breast tumors and normal breast tissues can be as high as 300% at a

laser wavelength of 1064 nm [9]. There are several reports related to photoacoustic imaging of small deeply embedded tumors, such as breast tumours [10-11].

Related applications have demonstrated that photocacoustic techniques have the ability to determine depth of port wine stain [12], and they have also been used to image blood vessels phantoms with high resolution [8].

Pulsed laser-induced thermal expansion in an absorptive structure in tissue creates ultrasonic transients by a thermoelastic mechanism. The induced PA waves propagate away from the source through the medium to be detected at some remote place by ultrasonic transducers. There is a wide range of transducers available, having been developed for the detection of laser-generated ultrasound [13]. Since photoacoustic (or laser-ultrasound) imaging is based on ultrasonic propagation and detection, it has the same spatial resolution capabilities as conventional imaging. The generation, propagation and detection of induced acoustic signals can be described by thermal expansion, wave equations and bandwidth filtering, respectively [5]. By directing the laser pulse onto a test sample, the absorbed optical energy in tissue is transformed into thermal energy, which is then, due to thermoelastic expansion, converted into mechanical stress. If the energy deposition occurs rapidly in a time period that is much less than the thermal relaxation time and the stress relaxation time, the local pressure rise after heating can be derived as $\Delta p = \frac{\beta c^2}{C_p} E_a$, where Δp is the pressure rise, β is the isobaric volume expansion coefficient, c is the speed of sound, C_p is the specific heat, and E_a is the absorbed optical energy density.

The behavior of photoacoustic waves is based on the following non-homogenous wave equation [14]

$$\nabla^2 p(r,t) - \frac{1}{c^2}\frac{\partial^2 p(r,t)}{\partial t^2} = -\frac{\beta}{C_p}\frac{\partial H(r,t)}{\partial t} \qquad (1)$$

where $p(\mathbf{r}, t)$ is the acoustic pressure at time t and position $\mathbf{r}$ and $H(\mathbf{r}, t)$ is the heat function of the optical energy deposited in the tissues per unit volume per unit time, which can be expressed as

$$H(r,t) = A(r)I(t) \qquad (2)$$

where $A(\mathbf{r})$ describes the optical energy deposition within the tissues at position $\mathbf{r}$ (structure of tissues); and $I(t)$ describes the shape of the irradiation pulse, which can be further expressed as $I(t) = \delta(t)$ for impulse heating. In term of photoacoustic tomography the objective is to reconstruct the distribution of the optical absorption $A(\mathbf{r})$ in the tissues from a set of measured acoustic signals $p(\mathbf{r}, t)$.

In this paper we have explored the potential for imaging a small object, obtaining photoacoustic images from several tissue samples. A key feature in this paper was the use of a polymer transducer used as a detector, integrated with a laser optical fibre delivery system. Another important feature to note is that the experiment was carried out in reflection mode, which offers a practical configuration for future clinical work.

THE PVDF PROBE

A polymer-based piezoelectric material, polyvinylidene fluoride (PVDF), was used in this study as an ultrasonic detector. The use of PVDF has been reviewed in several papers, for example Foster *et al* [15] and Lockwood [16]. Figure 1 illustrates a schematic diagram of the probe. The entire probe was based on a perspex shell with an outer diameter of 6.0 mm. With the PVDF adhered to the front face, silver-loaded epoxy was used as a backing material to support the transducer. The outer surface of the probe was painted with silver paint to provide an earth plane. Photoacoustic signals were extracted via a signal wire. A 0.5 mm hole was made at the centre of the probe, allowing an exit for an optical fibre, from which laser pulses were delivered. The thickness of the annular PVDF film was 28.0 μm.

The PA signal, and a corresponding frequency response of the probe when an aluminium sample was used as a target material is shown in Figures 2(a) and 2(b). Figure 2(a) shows that after an electrical noise pulse at time t = 2.0 μs, when the laser was triggered, the first photoacoustic pulse from the aluminium surface arrived at t = 8.3 μs. The Figure also shows a minimal ringing effect by the transducer system. An FFT of the photoacoustic pulse, shown in Figure 2(b), shows that the pulse had a maximum frequency response of ~ 5 MHz, with an extended high frequency response. Characteristics of received signals from a similar probe have been extensively studied [17-18]. Additionally potential applications for laser angioplasty and ophthalmology have also been demonstrated [19-22]. A similar type of probe was recently applied for NDT assessment [23-24].

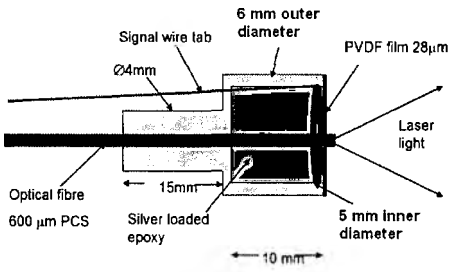

Figure 1: Cross-sectional view of the PVDF probe used in this project.

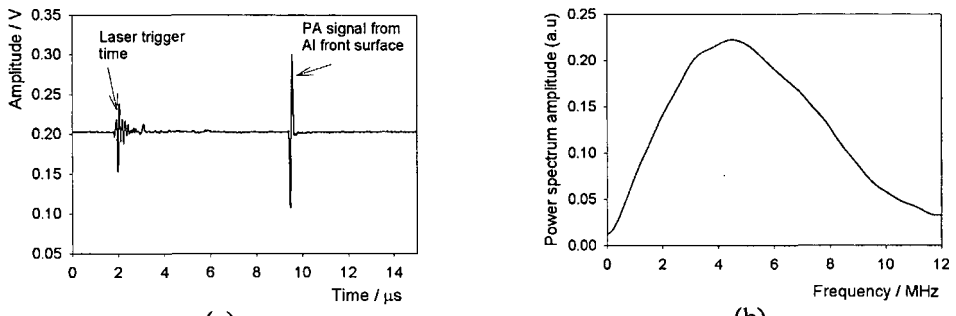

Figure 2: (a) A photoacoustic (PA) signals from aluminium sample showing a minimal ringing and (b). Pulse power spectrum of the probe from figure 2(a) showing a maximum frequency of ~ 5MHz, with an extended high frequency response.

EXPERIMENTAL ARRANGEMENT

The experimental arrangement for the photoacoustic system is shown in Figure 3(a). A Q-switched pulsed Nd:YAG laser, operating at a wavelength of 1064 nm, was used as the laser source. Laser pulse widths were ~8 ns with a pulse repetition rate up to 20 Hz. The beam was focused into a PCS optical fibre having a 600 μm core via a SMA connector, so that pulses could be delivered through the transducer head to the test sample. Figure 3(b) shows schematically a part of the scanning system with the sample under investigation. Any chicken breast sample was supported on a perspex base, with the whole system immersed in a saline solution. The PVDF probe was attached to a two-dimensional translation framework driven by step motors. It was designed to perform a linear scanning along a horizontal direction. In experiments reported here, both the transducer and the test sample were immersed in normal saline solution. This solution was prepared by dissolving 9.0g of sodium chloride (NaCl) in 1000 ml of distilled water.

Two cascade amplifiers of 20dB each amplified signals from the probe. A four channels digital oscilloscope (TDS-640A) was used to capture photoacoustic signals. It was addressed through a pc-computer with a program, under a Lab View® platform, that controlled both the scanning of the PVDF probe and data acquisition. This software had the capability to displaying A-scan signals or B-scan images.

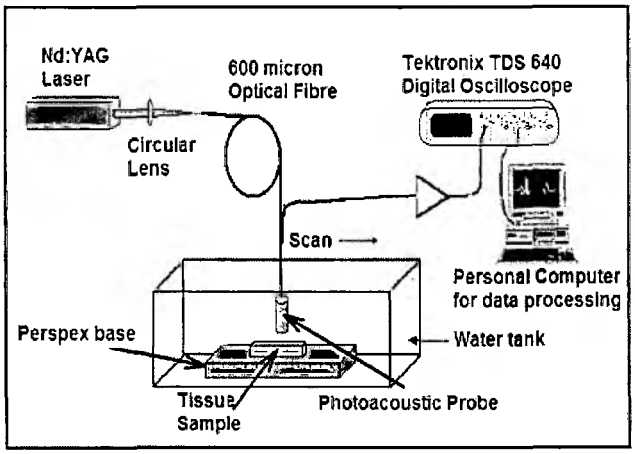

Figure 3(a): Experimental arrangement for the photoacoustic detection in backward mode

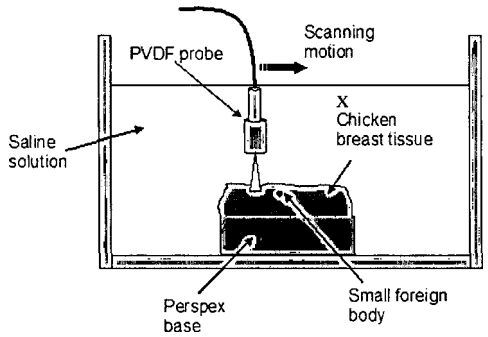

Figure 3(b): Close up diagram of foreign body in tissue sample from Figure 3(a).

SAMPLE PREPARATION

Test samples were prepared using fresh chicken breast. In several samples, a human hair or hairs were threaded into the chicken breast to act as a foreign body. Due to differences in optical absorption properties human hair with respect to tissue, high photoacoustic contrast between hair and chicken breast tissue was expected. In other samples, artificial hair made from nylon was used. It was very important to ensure that no air bubbles existed in the samples, since air bubbles strongly reflected acoustic signals. This risk was reduced by firmly pressing the chicken breast sample near the region where the hair had been threaded. Samples were fixed on a perspex block to make sure they did not move whilst scanning processes were performed.

Some experiments were also conducted when human or nylon hair was immersed directly in saline solution, held by side supports. These measurements helped to confirm that photoacoustic signals came from the foreign body and not from some other anomaly within the tissue sample.

RESULTS

Figure 4(a) shows a B-scan image from chicken breast tissue containing a strand of human hair to simulate a foreign body, near the surface of the chicken breast. Typical scanning parameters in our experiment were 150 steps with a spatial sampling interval in the x direction of 0.0625 mm per step. Horizontal and vertical axes in Figure 4(a) correspond to the transducer translation and depth into the chicken breast respectively. In the derivation of the depth axes, we used a sound velocity in chicken breast of 1500 m/s, similar to the speed of sound in soft tissue [25].

A feature labelled **A** in Figure 4(a) relates to an ultrasonic wave generated at the surface of the sample, which propagates back to the detector. An additional time delay within the water medium is not shown within the Figure. Signals from the hair are indicated as the feature labelled **B**. The curvature of such a feature correlates to the time delay of the propagating ultrasonic wave from the target to the detector at different positions. Fringes labelled **C** are believed to be due to ultrasonic resonance within the sample and will be discussed in later section of this paper.

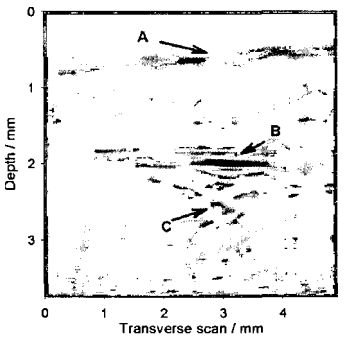

Figure 4(a): B-Scan of human hair in chicken breast showing (A) the chicken breast surface, (B) signals from the hair sample and fringes (C). An initial delay-time through the saline medium is not shown

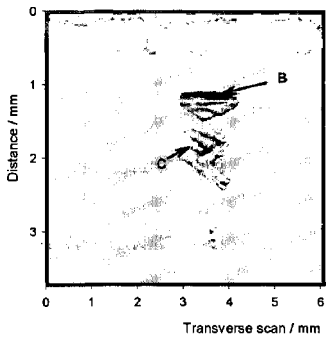

Figure 4 (b): B-Scan of human hair in normal saline solution showing (B) signal from the hair sample and fringes (C) . Delay signal from the detector to the surface was not shown

A similar hair sample was then placed directly in the saline solution and the scanning process was repeated to produce an image, Figure 4(b). An almost similar image was observed, except it was better defined compared to the one in chicken breast. The feature labelled **B** is the PA signal due to the hair sample, with **C** indicating a fringe region behind the initial photoacoustic signal. All signals in these experiments were averaged over 16 laser pulses.

DISCUSSION

It was interesting to note that during a scanning process, except for photoacoustic signals from the sample surface, there were normally no signals detected from the foreign body. Only as the combined probe moved above the top region of the sample containing the hair did additional signals become apparent. By performing a numerical cross-sectional measurement across the image, Figure 6(a) and 6(b), lateral resolution of the image taken at FWHM was determined to be ~500 μm and the depth resolution was measured to be ~80μm. These resolution limits may be compared with the real size of a human hair, of about 70 μm.

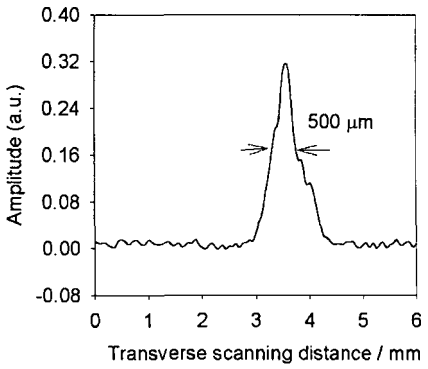

Figure 6(a): Lateral resolution of the probe measured across the image the hair

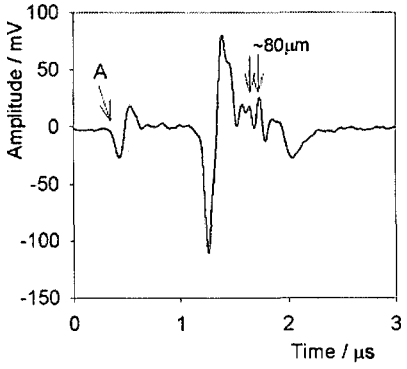

Figure 6(b): Depth resolution of the PVDF probe

Esennaliev *et al* [10] reported that the maximum depth for detection of spherical tumor phantoms of 2 mm diameter was 60 mm when using a forward mode configuration. In these present experiments involving human hairs in a backward reflection mode, with typical hairs of cylindrical diameter 60 -100 μm, we have shown results at depths down to 10 mm. This study demonstrates the capability of photoacoustic measurements to detect relatively small objects in tissue. Due to the finite size of the detector and the divergence of the laser beam within the solution, signals will be detected over an angular range of 11° as the detector moves across the sample. As a consequence there are secondary ultrasonic fringes in some B-scan images. They are more extensive when the absorbing site is further away from the probe, due to the geometry of the integrated probe.

It is evident from the 2-D image of Figure 4(a) that a fringe pattern occurs after the initial photoacoustic signal from the hair. To help understand this feature, it is essential to understand the anatomy of hair itself. A human hair shaft consists of three different

layers, namely the cuticle (the outer layer), the cortex and the central core called the medulla. Figure 7 schematically shows these layers as well as the overall diameter of the hair. The cuticle, having a thickness of ~1μm and being optically transparent, is unlikely to interact with incident laser pulses. On the other hand, both the cortex and the medulla have significant thickness and colour that contribute to optical absorption of laser pulses, thus inducing acoustic waves across its diameter. It is suggested that the fringe features may be due to an ultrasonic resonance effect within the hair sample.

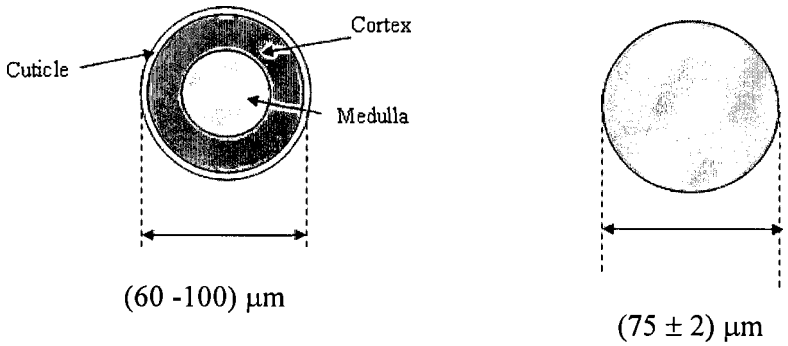

Figure 8: Schematic diagram showing cross section of human hair and nylon

To explore this possibility, further experiments were conducted using an artificial monofilament nylon hair in place of a human hair. Other parameters of the experiment remained the same as before. The advantages of using artificial hairs were they were less complex and had a similar diameter to human hair. The experiment was conducted within chicken breast to provide a resulting image shown in Figure 8(a). The scan revealed an image of the artificial hair similar to the ones with human hair, with the exception of fringes behind the initial image that appeared to be more uniform. In this image, the feature labelled **G** was the chicken surface, **H** was a signal due to the artificial nylon hair, and **I** were fringes similar to **C** in Figure 4(a). A-scans of a nylon hair in saline were also captured, with typical results shown in Figure 8(b). It is interesting to see a degree of uniformity in these waveforms. They show a series of photoacoustic signals, almost identical in shape, and decaying exponentially with time. From several experiments showing repeatability, we note that acoustic resonance effects within artificial nylon hair made in the form of a single filament are likely to have a more regular time domain behaviour due to structural homogeneity across the fibre diameter.

Using a typical A-scan signal for the artificial hair as depicted in Figure 9(b), the time difference, Δt, between peaks was measured as ~ 0.08 μs. This is the elapse time for ultrasound to travel twice the diameter of the nylon. Micrometer measurement of the nylon diameter was 75 μm. Consequently, the velocity of nylon was calculated using the formula, $v = 2d/\Delta t$, where d is the diameter of the nylon and Δt is the time difference between two neighbouring peaks. The velocity in nylon was found to be (1875 ± 72) m/s. This value was is well within the accepted range of nylon velocities, (1600 – 2600) m/s [26]. This evidence suggests that from a photoacoustic interaction, the fringes are associated with ultrasonic pulses resonating within the structure of the sample.

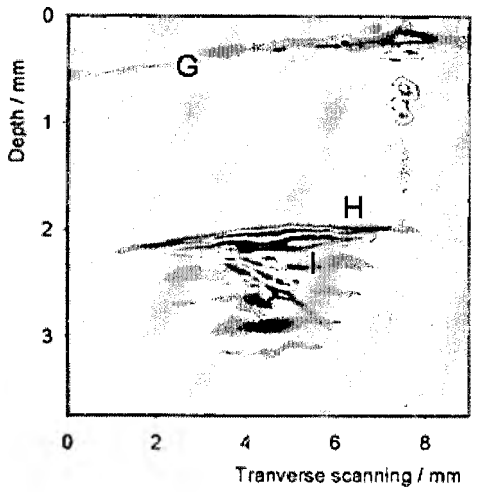

Figure 9(a): B-Scan of artificial nylon hair in chicken breast

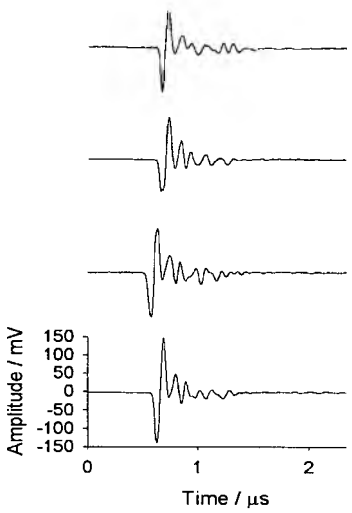

Figure 9(b): A typical A-Scan of artificial nylon hair in normal saline solution showing evidence of resonance decaying in exponential mode.

CONCLUSIONS

In this study we have demonstrated the capability of a photoacoustic technique for imaging a small object embedded within tissue. With a typical diameter of 70μm, a human hair within tissue has been detected down to a depth of 10 mm. Using a one-dimensional scanning system, photoacoustic images have not only shown the presence of such foreign bodies within tissue, but they have also contained photoacoustic features that may indicate the cross-sectional dimension of hair-like filaments. The evidence suggests that from photoacoustic interactions on the filaments, fringes in a B-scan are associated with ultrasonic pulses resonating within the structure of the hair. The present lateral resolution of ~500 μm is restricted by the finite sensor area together with the laser beam divergence from the probe head. Depth resolution is currently at ~80 μm for the present transducer probe. A photoacoustic probe of the type described in this paper may have future applications in the field of medical diagnosis.

ACKNOWLEDGEMENT

We wish to acknowledge financial support from University Technology of Malaysia and the Government of Malaysia for Jasman Zainal. During the course of this work, we also acknowledge Dr S Boonsang for his help in software development for the production of photoacoustic images, and for his general assistance.

REFERENCES

[1] Warner E., P. D. B., Shumak R. S., Catzavelos G. C., Di Prospero L. S., Yaffe M. J., Goel V., Ramsay E., Chart P. L., Cole D. E.C., Taylor G. A. , Cutrara M., SamuelsT. H. , Murphy J. P., MurphyJ. M., Narod S. A., (2001). "Comparison of Breast Magnetic Resonance Imaging, Mammography, and Ultrasound for Surveillance of Women at High Risk for Hereditary Breast Cancer." Journal of Clinical Oncology **19**(15 (August)): 3524-3531.

[2] Tam A.C. (1986). "Applications of photoacoustic sensing techniques." Rev. Mod.Phys **58**(2): 381-431.

[3] Karabutov A.A., P. N. B., Letokhov V.S., (1996). "Time-resolved laser opto-acoustic tomography of inhomogenous media." Applied Physics B **63**: 545-563.

[4] Karabutov A.A., S. E. V., Podymova N.B., Oraevsky A.A, (2000). "Backward mode detection of laser-induced wide-band ultrasonic transients with optoacoustic transducer." J. Appl. Phys **87**(4): 2003-2014.

[5] Ku G., W. L. V. (2000). "Scanning thermoacoustic tomography in biological tissue." Med.Phys. **27**: 1195-1202.

[6] Oraevsky, A.A., Jacaques, S.L. and Tittel, F.K. (1997) "Measurement of tissue optical properties by time-resolved detection of laser-induced transient stress." Applied Optics, 36,402-415.

[7] Hoelen C.G.A. (2001). "Detection of Photoacoustic Transients Originating form microstructures in Optically Diffuse media such as in biological tissue." IEEE Transaction on Ultrasonics,Ferroelectrics and Frequency Control **46**(1): 37-47.

[8] Hoelen C.G.A., d. M. F. F. M., Pongers R., Dekker A., (1998). "Three-dimensional photoaoustic imaging of blood vessel in tissue." Optics Lett. **23**: 648-650.

[9] Oraevsky A.A., A. V. G., Karabutov A.A., Esenaliev R.O. (1999). 2-D Opto-Acoustic Tomography Transducer array and Image reconstruction Algorithm. SPIE Conference on Laser tissue Interaction X : Photochemical,Photothermal and Photomechanical, San Jose, California, SPIE.

[10] Esenaliev R.O., K. A. A., Oraevsky A.A, (1999). "Sensitivity of laser opto-acoustic imaging in detection of small deeply embedded tumors." IEEE Quant.Electr. **5**(4): 981-988.

[11] Oraevsky A.A., K. A. A., Solomatin S.V., Savateeva E.V.,Andreev V.G., Gatalica Z., Singh H., Fleming R.D., (2001). Laser optoacoustic imaging of breast cancer in vivo. Proc SPIE, 4256, 6-15.

[12] Viator, J. A., Au,G., G. Paltauf, S.L. Jacques, S.A. Prahl, H.W.Ren, Z.P. Che and J.S. Nelson, (2002). "Clinical testing of a photoacoustic probe for port wine stain depth determination,." Lasers Surg Med. **30**: 141-148.

[13] Dewhurst R.J. and Shan Q., (1999) "Optical remote detection of ultrasound" Measurement Science and Technology, 10, R139-R168.

[14] Gusev V.E, K. A. A. (1993). Laser Optoacoustic. New York, American Institute of Physics.

[15] Foster F.S., H. K. A., Sherar M.D., (2000). "A history of medical and biological Imaging with Polyvinylidene Flouride (PVDF) transducers." IEEE Trans. on Ultrasonics, Ferroelectrics and Frequency Control., **47**(6): 1361-1371.

[16] Lockwood G.R., F. F. S. (1994). "Modelling and optimization of high-frequency ultrasound transducers." IEEE Transaction on Son.Ultrason. **SU-41**: 225-230.

[17] Shan Q., K. A., Payne P.A., Dewhurst R.J., (1996). "Characterisation of laser-ultrasound signals from an optical absorption layer within a transparent fluid." Ultrasonics **34**: 629-639.

[18] Roome K.A., Payne P. A., Dewhurst R.J., (1999). "Towards a sideways looking intravascular laser-ultrasound probe." Sensors and Actuators **76**: 197-202.

[19] Chen Q.X., D. A., Dewhurst R.J., and Payne P.A., (1993). "Photoacoustic probe for intra-arterial imaging and theraphy." Electronic Letter **29**: 1632-1633.

[20] Roome K.A., Caller R.F., Payne P.A. and Dewhurst R.J. (1998) "Laser-ultrasound tissue characterization methods for potential use in laser angioplasty", Nondestructive Characterization of Materials VIII, Plenum Press, 105-110.

[21] Payne P.A., Sadr A., Rosen E.S., and Dewhurst R.J. (2000). "Ophthalmic applications of laser-generated ultrasound." Proc. SPIE, 3908, 13-22.

[22] Sadr A., Payne P. A., Rosen E.S., Dewhurst R.J. (2000). "Laser-Generated Ultrasound within the eye." Acoustical Imaging, vol 25, 549-554, Kluwer Academic/Plenum Publishers.

[23] Boonsang, S., Zainal, J.,Dewhurst,R.J., (2004a). "Synthetic aperture focusing techniques in time and frequency domains for photoacoustic imaging." Insight **46**(4): 196-199.

[24] Boonsang S., Zainal J. and Dewhurst R.J. (2004b) "Photoacoustic imaging using a frequency domain synthetic aperture focusing technique." Proc SPIE, 5486, 267-273.

[25] Wang, M. X. a. L. V. (2003). "Analytic explanation of spatial resolution related to bandwidth and detector aperture size in thermoacoustic or photoacoustic reconstruction." Phys Rev **67**,(056605): 1-15.

[26] Krautkramer J., K. H. (1990). Ultrasonic testing of materials. New York, Springer-Verlag.

